JOURNAL OF APPLIED ELECTROCHEMISTRY 15 (1985) 325–334

Analysis of the principal component of external casing corrosion in deep wells

LEENDERT de WITTE

PO Box 1294, San Ysidro, California, CA 92073, USA

Received 4 January 1984; revised 15 May 1984

One of the most general causes of severe external casing corrosion in deep wells is the effect of spontaneous electrochemical potentials generated by the concentration contrasts between the connate formation waters and the drilling mud. These potentials are registered on the open hole electrical well logs as the so called S.P. curve.

The S.P. currents caused by the spontaneous potentials in the electrically conductive environment near the intersection of formation boundaries with the drillhole are short-circuited by the introduction of casing in the hole and the effects of the numerous cells are superimposed along the length of the casing. The anodes of the resulting system of currents are the critical areas of external corrosion.

The quantitative theory for the computation of the anodic current densities and the corresponding external iron loss was derived by the author in 1955. The present article gives excerpts of the theory of the spontaneous potentials, S.P. currents and their superposition along the casing. Significant improvements are introduced in the numerical analysis leading to the digital computation of the iron-loss profiles. A field example is given for one of the geothermal wells in the Cerro Prieto field in Baja California, Mexico, showing pitting depth penetrations of up to 1 mm per year which suggests a casing failure span of around fifteen years for unprotected pipe.

The present approach can be expanded directly or by the use of finite element computational techniques to take into account effects of casing cement and cathodic polarization. Such extension would lead to meaningful prognostication of cathodic protection current requirements for individual wells.

1. Introduction

For the last half century almost all drilling of deep holes has been done with rotary drilling equipment. In this process the rock chips cut out of the formations by the rotary drill bit are carried to the surface by a circulating viscous mud slurry. In the majority of cases these muds are made up of available surface waters and pulverized clay minerals of the montmorillonite–bentonite class, with barite as a weighting agent. As in the deeper strata the connate formation waters, not flushed by groundwater movement, are normally of appreciable degrees of salinity, an ionic concentration contrast exists between the drilling fluid in the borehole and the connate waters in the horizons that are penetrated.

These concentration contrasts give rise to a variety of electrochemical diffusion potentials which, in the conductive surroundings, cause currents to flow around the points of intersection of the bore-hole with the different formation boundaries. The ohmic drops of these currents in the mud column were noticed by the early operators of electric resistivity logging devices (*carottage électrique*) in the Baku oilfields. Soon the diagnostic correlation of these ohmic 'spontaneous' potential drops with formation and connate water characteristics were realized and the potentials measured against a remote surface reference electrode were recorded as a separate curve, the so called Spontaneous Potential or S.P. curve on the electric bore-hole logs. The currents occasioning the ohmic drops are referred to as S.P. currents.

When casing is set in a drillhole, the metal pipe short-circuits the S.P. currents and the effects of the many cells are superimposed along the length of the pipe. The current variations along the pipe corre-

0021–891X/85 $03.00 + .12

spond to anodic and cathodic areas, where positive current leaves or enters the metal. The strongly anodic regions are the locations of the most severe external corrosive attack on the casing.

The open hole recording of the S.P. curve gives us the basic data, for any particular hole, for deriving by the techniques of mathematical physics, the resulting current distribution in the pipe once casing is set. The evaluation of the analytical expressions for the casing current distribution obtained by the application of potential theory and linear transform theory, is done by digital computation and requires a considerable amount of numerical analysis. Based on the analytical presentation of the S.P. currents by Doll [1], the theory of the casing corrosion current distributions was developed by the author in response to a question by Radd regarding a possible connection between the S.P. and external casing corrosion [2]. An improved numerical approach for the computational procedure was added by de Witte and Fournier [3]. Iron loss rates prognosticated from computed anodic current densities compared spectacularly with direct measurements on pulled casings in the San Miguelito oil field in California [4]. The current paper reviews the electrochemistry of the S.P. phenomena, presents the theory of the casing current distribution, adding a number of mathematical improvements and gives a field example for a well in the geothermal field of Cerro Prieto in Baja, California.

2. Spontaneous potentials

Where the filtrate of the drilling mud makes contact with the connate water in electrochemically inert formations such as clean sandstones and limestones, the concentration contrast leads to the establishment of simple liquid–liquid junction potentials. On the other hand, where the ionic diffusion takes place through endurated pure shales which because of the fixed negative charges on the clay mineral lattices are permeable to positive ions only, the formation of Nernst potentials results.

The liquid junction potentials are given by

$$E_1 = \frac{RT}{F}\left(\frac{u-v}{u+v}\right)\ln\frac{\alpha_w}{\alpha_{mf}} \tag{1}$$

and the Nernst potentials by

$$E_2 = \frac{RT}{F}\ln\frac{\alpha_w}{\alpha_{mf}} \tag{2}$$

where R, T and F have their usual meanings, u and v are the mobilities of the positive and negative ions, respectively, for the simple case of a 1–1 electrolyte; α_w and α_{mf} are the electrolyte activities of the connate water and the mudfiltrate.

For NaCl solutions at 75° F, these expressions reduce to

$$E_1 = -11.5\log\frac{\alpha_w}{\alpha_{mf}} \simeq -11.5\log\frac{R_{mf}}{R_w} \quad \text{(mV)}$$

$$E_2 = +59.1\log\frac{\alpha_w}{\alpha_{mf}} \simeq +59.1\log\frac{R_{mf}}{R_w} \quad \text{(mV)}$$

R_{mf} and R_w are the electrical resistivities of the mudfiltrate and connate water, respectively.

The potential difference between the mud column in front of a thick clean sandstone and that in front of an adjacent thick pure shale will therefore be under the indicated conditions

$$E_{SP} \simeq -70.6\log\frac{R_{mf}}{R_w} \quad \text{(mV)} \tag{3}$$

This equation is one of the fundamental relations in quantitative electric log analysis for clean formations. If the porous strata contain disseminated clay particles, as is the case for so-called 'shaly sands', the liquid junction potentials established between the mudfiltrate and the connate waters take the form of imperfect membrane potentials. The electrochemical interpretation of such potentials was first given

by Teorell [5] and by Meyer and Sievers [6]. In the resulting quantitative expressions appear an additional parameter, namely, the average concentration of fixed negative clay lattice charges in the interstitial volume, denoted by m_r. Taking into account the reduced ionic activity of the counter ions associated with the fixed lattice charges, de Witte [7] derived an approximate expression for the S.P. in shaly water sands in the form:

$$E_{SP} \simeq -70.6 \log \frac{m_r + 2.5 m_w}{m_r + 2.5 m_{mf}} \tag{3a}$$

where the ionic concentrations m_r, m_w and m_{mf}, respectively, of the fixed lattice charges, the connate water and the mudfiltrate are expressed as molalities.

In the practical electric log interpretation techniques, further corrections are made for ionic contents differing from that of NaCl solutions and for the deviations from simple inverse proportionality in the relation between electrolyte activity and electrical resistivity.

3. S.P. currents

The quantitative relation between the double layer e.m.f.s of the diffusion potentials and the ohmic drops in the mud column, due to the resulting S.P. currents, was given by Doll of the Schlumberger Corporation [1]. In the mathematical presentation of Doll's treatment and that of the subsequent sections on casing current distributions the following nomenclature will be used:

The Laplace equation:
Cylindrical coordinates: ϕ, r and z

ϕ = angular measure in plane perpendicular to z-axis
z = vertical distance along axis of hole; positive upward
r = radial distance from axis of hole
V = electrical potential
k = variable of integration
$\alpha(k)$, $\beta(k)$ = functions of the variable of integration, depending on the radii of the cylindrical boundaries and the resistivity contrasts across these boundaries.

Resistivities:

R_t = average formation resistivity (Ωm)
R_m = mud resistivity or equivalent resistivity inside the drill hole (Ωm)

$$a \equiv \frac{R_t}{R_m} - 1$$

Modified Bessel functions:

I_0 = modified Bessel function of the first kind and zero order
I_1 = modified Bessel function of the first kind and first order
K_0 = modified Bessel function of the second kind and zero order
K_1 = modified Bessel function of the second kind and first order
$M(p) \equiv pK_0(p)K_1(p)$
$Q(p) \equiv pK_0(p)I_1(p)$

Potential in drill hole due to ionic double layers:

W_0 = one half of the potential difference on the axis of the hole, between points at both sides of a sand–shale interface and at a large distance of the interface (half of the 'static' S.P. of Equation 3)
W_z = potential along the axis of the hole, due to a single sand–shale interface, as a function of z

Superposition theorem:

$f_i(z)$ = input potential distribution as function of z

$\hat{f}_i(z)$ = input current distribution as a function of z

$f_r(z)$ = response or output potential distribution as function of z

$\hat{f}_r(z)$ = response or output current distribution as function of z

$f_r^*(z)$ = response to the input of a unit step function in the potential along the axis of the hole

$$R(z) \equiv \frac{df_r^*(z)}{dz}(2\pi)^{1/2}$$

$$R'(z) \equiv \frac{d^2f_r^*(z)}{dz^2}(2\pi)^{1/2}$$

Special parameters and expressions used in the numerical analysis

p = variable of integration

Δp = step size of p for numerical integration in a given interval

$F(p)$ = non-circular part of integrand of the definite integral in the expression for the current resulting from a unit step function input (Equation 8)

$F'(p) \equiv F(p) - p^2K_1(p)$

$\Gamma(n)$ = gamma function; $\Gamma(n+1) = n\Gamma(n)$ for $n > 0$

$\Gamma(n+1) = n!$ for n integer

With the above definitions and nomenclature we now present Doll's derivation of the quantitative expression for the S.P. currents, starting with the potential distribution around a point charge in the hole. The latter is found as a solution of the Laplace equation in cylindrical coordinates:

$$\frac{\partial^2 V}{\partial r^2} + \frac{1}{r}\frac{\partial V}{\partial r} + \frac{1}{r^2}\frac{\partial^2 V}{\partial \phi^2} + \frac{\partial^2 V}{\partial z^2} = 0$$

As long as cylindrical symmetry prevails, V is independent of the angle ϕ so that $(\partial^2 V/\partial\phi^2) = 0$.

By the method of separation of variables one obtains for the general solution:

$$V = \int_0^\infty \{\alpha(k)I_0(kr) + \beta(k)K_0(kr)\}\cos(kz)\,dk \tag{4}$$

The derivation proceeds by observing that the potential due to a semi-infinite double layer at the boreface, for all points enclosed by it, is equal to that of a double layer disc perpendicular to the boreface and closing off the cylindrical boundary. Upon differentiating Equation 4 with respect to z to reflect the dipole nature of the double layer, using the reciprocity theorem for exchanging the roles of point source and potential at a point and integrating over the area of the disc, Doll finds for the potential on the axis of the hole due to a single sand–shale interface the expression:

$$W(z) = W_0\left[1 + \frac{z}{(1+z^2)^{1/2}} - \frac{2}{\pi}\int_0^\infty A(p,a)I_1(p)\sin(pz)\,dp\right] \tag{5}$$

where $A(p,a) = [apK_0(p)K_1(p)]/[1 + apK_0(p)I_1(p)]$.

The S.P. currents in the hole are proportional to the voltage gradient (dW/dz). The open hole electric logs recorded the ohmic drops of these currents in millivolts as a function of depth as the Spontaneous Potential or S.P. curve. Fig. 1a gives an example of a portion of the S.P. curve for a typical well in the geothermal field of Cerro Prieto, Baja California, Mexico.

4. Casting currents

When casing is set in the hole the S.P. currents are short-circuited. The resulting currents in the pipe as a function of depth, $\hat{f}_r(z)$, are considered as a distortion of the system of currents in the open hole, $\hat{f}_i(z)$,

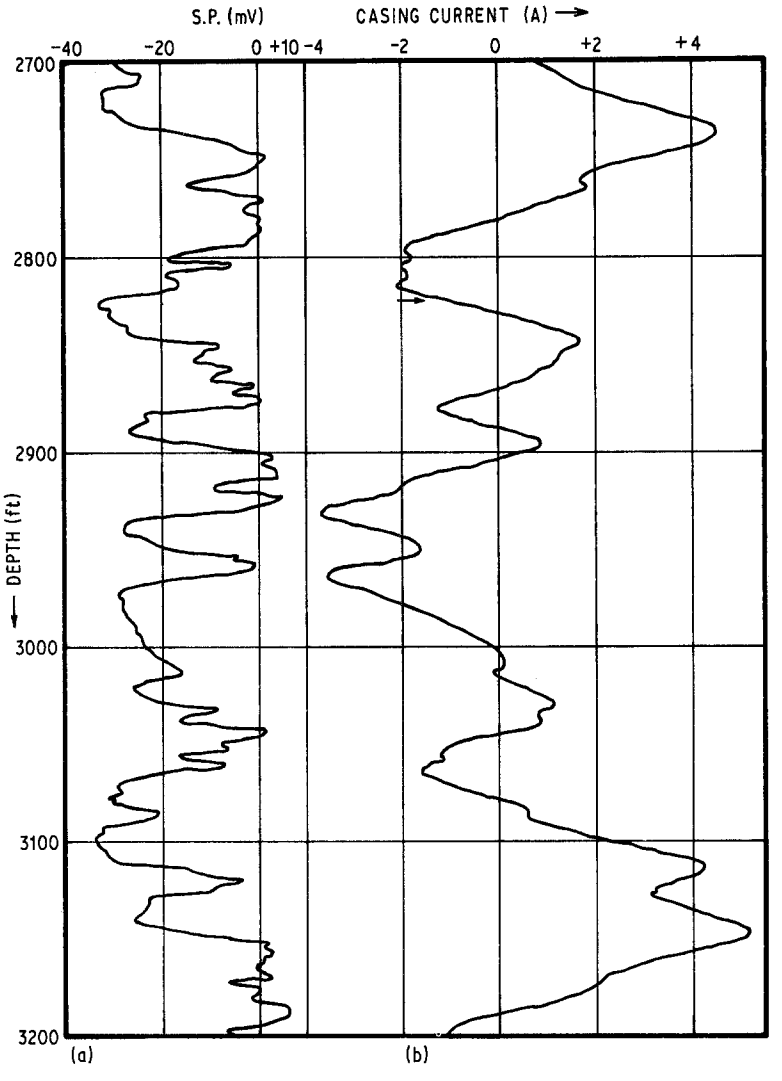

Fig. 1. (a) S.P. (mV) vs depth (ft) for Well Number M-5 in geothermal field of Cerro Prieto Baja California Norte, Mexico; (b) Casing current (A) vs depth (ft): Positive current upwards = +; positive current downwards = −.

or rather the corresponding potentials $f_r(z)$ are taken as a distortion of the input potentials, $f_i(z)$, registered as the open hole S.P.

The relation between the resulting distribution $f_r(z)$ and the input $f_i(z)$ is given by the superposition theorem of linear transform theory, also known as Duhamel's theorem, in the following form:

$$f_r(z) = \frac{1}{(2\pi)^{1/2}} \int_{-\infty}^{\infty} f_i(y) R(z-y)\, dy \tag{6}$$

where $R(z) = (df_r^*(z)/dz)(2\pi)^{1/2}$ and $f_r^*(z)$ is the response of the system to the input of a unit step-function, i.e. for $f_i(z) = 1$ when $z > 0$ and $f_i(z) = 0$ for $z < 0$.

This response to a unit step-function in potential is given precisely by Equation 5, with $W_0 = 0.5$ and substituting for R_m a resistivity which gives an electrical resistance per metre length of the hole equal to the longitudinal resistance of one metre of the casing.

As we are more interested in the distribution of casing currents than in that of the potential, we form the derivative

$$\frac{df_r(z)}{dz} = \frac{1}{(2\pi)^{1/2}} \int_{-\infty}^{\infty} f_i(y) R'(z-y)\, dy \tag{7}$$

where $R'(z) = (dR/dz) = [d^2 f_r^*(z)/dz^2](2\pi)^{1/2}$.

The double differentiation of Equation 5 gives

$$\frac{1}{(2\pi)^{1/2}} R'(z) = W_0 \left[\frac{-3z}{(1+z^2)^{5/2}} + \frac{2}{\pi} \int_0^\infty pA(p,a) I_1(p) \sin(pz)\, dp \right] \tag{8}$$

The numerical integration of Equation 7 is carried out by the Trapezoid rule, after first establishing a tabulation of $R'(z)$ as a function of z and is repeated for all values of z, over the length of the hole, in order to obtain the current profile in the casing.

The computation of Expression 8 is much more complicated, due to the fact that the rapid oscillations of sin (pz) for most of the values of the argument, make direct numerical integration impractical over the larger part of the integration interval.

5. Numerical analysis

A fairly efficient method for the evaluation of integrals of the type occurring in Equation 8, was presented by de Witte and Fournier [3]. The essence of this method and a number of significant improvements developed in the course of the current research are now described.

The basic idea of the procedure is to divide the non-circular part of the integrand, which we denote by the function $F(p)$, into a number of intervals and to approximate $F(p)$ in each interval by a simpler function whose product with sin (pz) can be integrated formally. In the central intervals fourth order polynomials were used to approximate $F(p)$, while for $p \ll 1$ and for $15 < N < p < \infty$ the low order terms of the asymptotic expansions of the modified Bessel functions were combined into relatively simple expressions. The precision of the polynomial approximations was monitored by means of small triangles whose apices were formed by the difference between the approximation and the true value of $F(p)$, and whose contributions to the total integral were determined and listed separately with the digital results. If the summed contributions of the error triangles was judged to be too large, the size of the intervals was reduced. In the present work several improvements, both in efficiency and precision, are introduced especially in the processing of the asymptotic ends of the integrand and the computations for very large values of z.

A considerable simplification was achieved by substituting a continuation of the polynomial approximations in place of the asymptotic expansions, for small values of the argument. Such substitution is permissible in view of the fact that $F(p)$ goes to zero for $p \to 0$. For values of $pz \ll 1$, however, there occurs a very severe mutual cancellation between the values of the integrated expressions for the products of the individual polynomial terms and sin (pz), to such extent that even using double precision, one is left with an insufficient number of significant figures in the result. To eliminate this difficulty, simple numerical integration was introduced for the intervals with $p_{\max} z < \pi/4$, where the integrand increases monotonously. As the step size, Δp, is constant in each interval, the five point Newton–Cotes method was selected, which is given by:

$$\int_{x_0}^{x_4} f(x)\, dx = \frac{2\Delta x}{45} (7f_0 + 32f_1 + 12f_2 + 32f_3 + 7f_4)$$

Another major simplification was made in the interval $p > N > 15$, based on the following sequence of considerations: The function $F(p)$ can be written in the form

$$F(p) = \frac{ap^2 M(p)}{1 + aQ(p)} I_1(p)$$

For large values of p we have the asymptotic expansion:

$$Q(p) = 1/2 \left[1 - \frac{1}{2p} - \frac{(1)^2 3}{2(2p)^3} - \frac{(1)^2 (3)^3 5}{2(2p)^5} - \cdots \right]$$

which shows that $Q(p)$ tends towards 1/2.

For 8″ casing (20.3 cm) and $R_t = 5$ ohm m, the parameter 'a' is of the order of 10^5 so that $aQ(p) \gg 1$ and therefore in the interval under consideration $F(p) \to p^2K_1(p)$.

At this point we use one of the integral transforms of Erdelyi *et al.* [8]:

$$\int_0^\infty p^2K_1(p)\sin(zp)\,dp = 2(\pi)^{1/2}\Gamma\left(\frac{5}{2}\right)z(z^2+1)^{-5/2} \tag{9}$$

We now write:

$$\int_N^\infty p^2K_1(p)\sin(zp)\,dp = \int_0^\infty p^2K_1(p)\sin(zp)\,dp - \int_0^N p^2K_1(p)\sin(zp)\,dp$$

This means that in the interval 0–N we can change the non-circular part of the integrand, $F(p)$ to $F'(p)$, where:

$$F'(p) = p^2\left[\frac{M(p)I_1(p)}{1+aQ(p)} - K_1(p)\right]$$

and add to the resulting integral the closed form expression of Equation 9, thus eliminating entirely the quite laborious evaluation of the integrals of the asymptotic expansion terms multiplied by sin (zp) for the interval $N < p < \infty$.

Furthermore, considering that for the Gamma function we have $\Gamma(n+1) = n\Gamma(n)$, for $n > 0$ and $\Gamma(\frac{1}{2}) = (\pi)^{1/2}$, the closed form expression: $2(\pi)^{1/2}\Gamma(5/2)z(z^2+1)^{-5/2}$, becomes $\pi/2.3z(1+z^2)^{-5/2}$, thereby cancelling precisely the algebraic part (the first term on the right hand side) of Equation 8.

With this set of simplifications Equation 8 reduces to:

$$\frac{1}{(2\pi)^{1/2}}R'(z) = W_0\left[\int_0^N F'(p)\sin(zp)\,dp\right] \tag{10}$$

where N satisfies the condition: $aQ(N) \gg 1$.

The values of $R'(z)$ start at zero for $z = 0$, pass through a maximum at a value of z smaller than unity and then decay exponentially as z increases.* For $z > 500$, the magnitude of $R'(z)$ has been reduced to such extent that effects of the errors of approximation become noticeable. One is apprised of this fact by the magnitude of the contribution of the error monitoring triangles to the final result. Fortunately for these high values of z, the function $R'(z)$ becomes inversely proportional to z, a fact which can be observed empirically and is verified theoretically in the following manner:

The function $F'(z)$ can be represented by the sum of a polynomial $P_n(p)$ of degree n and an exponential of the form $\alpha e^{-\beta p}$. It can be demonstrated that the definite integrals, between the limits zero and $2\pi M/z$, where M is an integer of any size, of the product $P_n(p)\sin(zp)$, are inversely proportional to z. Similarly we have: $\int_0^{2\pi M/z}\alpha e^{-\beta p}\sin(zp)\,dp \sim z/(z^2+\beta^2)$, which for z sufficiently large approaches $1/z$.

In the entire analysis presented here the unit length is taken as the radius of the hole. This means that if we wish to read the S.P. input in steps of 2.5 ft and perform the numerical integration of Equation 7 with the same step size, we must compute and tabulate $R'(z)$ in increments $\Delta z = 7.5$ in the case of an eight inch casing where one foot equals three hole radii.

The parameter 'a' is a function of the average formation resistivity, R_t, and the resistance per unit length of casing and changes therefore with the diameter and wall thickness as well as with the metallurgical composition of the casing.

6. Field example

Fig. 1a shows a section of the S.P. log for Well No. M-5 in the geothermal field of Cerro Prieto in Baja California, Mexico. In this graphical recording the average shale base-line was taken as the reference zero. A parallel displacement of this line does not affect the casing current calculations.

* A typical example of the general form of $R'(z)$ as a function of z, is given in Fig. 7 of [2].

The computed casing current profile for the same depth interval is shown in Fig. 1b. Where positive current diminishes upwards, it is leaving the pipe. This means that the corresponding area is anodic and a locus of external casing corrosion. In the interval depicted, significant anodic areas occur at the following depths: 2700–2735; 2817–2842; 2877–2895; 2935–2950; 2965–3030; 3060–3115 and 3127–3147. The corrosive current densities in these zones can be calculated from the formula:

$$i_c = \frac{I(z + \Delta z) - I(z)}{\pi d \Delta z} \tag{11}$$

where the current density i_c will be in $A\,cm^{-2}$ when the casing current, I, is taken in amperes while the depth differential, Δz, and the external casing diameter, d, are expressed in cm.

As shown in [4] the resulting iron loss per year is found using Faraday's law and the following conversions; $1\,mA = 10^{-3}\,C\,s^{-1} = 86.4\,C\,day^{-1} = 31\,536\,C\,yr^{-1} = 9.125\,g\,yr^{-1}$. We assume here that all of the iron goes into solution as ferrous ions. From the iron loss per cm^2 given in $g\,cm^{-2}$ we find the depth of iron removal or corrosive penetration, dividing by the metal density ($g\,cm^{-3}$), which yields: $1\,mA\,cm^{-2} \rightarrow 1.2\,cm\,yr^{-1}$.

In the current profile for the interval of Fig. 1, the steepest anodic slope occurs at a depth of 2820–2822.5 ft, where the computer output listed a decrease of positive current of 505 mA per 2.5 ft. For an external casing diameter of $11\frac{3}{4}''$ this corresponds to a current density of $0.071\,mA\,cm^{-2}$ or to a depth of corrosive iron removal of 0.85 mm per year. For a wall thickness of $\frac{1}{2}''$ this would mean total failure of unprotected pipe, without cement, in about fifteen years. Stresses and internal pressure on the pipe will accelerate the failure, as does the superposition of galvanic pitting on the corrosion profile we have described. The distribution and magnitude of galvanic effects due to inhomogeneities in the surface layers of the casing steel can be studied by running inside casing S.P. surveys [4]. These effects seem in general to be of shorter duration than the S.P. current corrosive mechanism and therefore play a subsidiary role in failure prognostication. As mentioned before iron loss calculations from S.P. casing current profiles in the San Miguelito oil field of Ventura County, California, carried out in a cruder, less precise form than that of the methodology described in this study, showed consistent agreement with the iron loss measured directly on pulled casing strings [4].

In contrast to the galvanic effects which increase the casing failure rate, properly bonded cement sheaths and polarization of the cathodic areas of the pipe will tend to slow down the corrosive penetration. For the order of current densities under consideration the cathodic polarization or hydrogen overpotentials in anaerobic environments act as an added electrical resistance per unit surface area of the pipe. Similarly a homogeneous well bonded cement sheath forms a cylindrical layer of additional resistance to current flow in the annular space between the casing and the boreface. Both of these factors can be incorporated in our analytical model by using multiple concentric cylindrical boundaries in the derivation of the potential distribution due to the S.P. dipole layers. The essential mathematics for the solution of the multiple boundary problem is that used in the computation of the resistivity departure curves, used in quantitative electric log interpretation and was described in detail by Frankel *et al.* [9].

The treatment of uneven cement bonding, strong variations in formation resistivities, multiple casing strings and other vertical discontinuities is preferably carried out using finite elements numerical techniques.

As a final spectacular example of the mechanism of casing corrosion by the shortcircuiting of S.P. type electrolyte concentration potentials, we mention the casing failures in the N.W. Burnett oil field in Ellis County, Kansas. Here the relatively fresh water bearing Dakota sandstones lie stratigraphically above the Wellington Salt section. The diffusion and shale membrane permeability effects cause the fresh water sands to be positive with respect to the halite and the salt saturated mud column. When pipe is set, positive current enters the casing opposite the Dakota sands and leaves in the upper part of the salt section, where it produces disastrous iron losses and consequent casing failures.

It is also of interest to observe that while borehole spontaneous potentials are ubiquitous, the rates of

external casing corrosion vary considerably from region to region. The absence of severe casing corrosion may be due to various factors. In limestone areas extremely hard and resistive scales are frequently deposited at the cathodic regions of the pipe, strongly reducing the intensity of the corrosion currents. In many other fields, especially at the edges of sedimentary basins, moving ground waters replace the mud columns in the annulus around the casing within months of completion of the wells thus removing the cause of the spontaneous potentials. A good example of this is found in the Los Angeles Basin fields, which have by and large the same Pliocene and Miocene stratigraphic section as the fields in Ventura County and generally do not suffer severely damaging external casing corrosion rates.

7. Cathodic protection requirements

The objective of cathodic protection is to apply to the structure under consideration and its environment an electric current system in which the former is the cathode, i.e. a system in which, considered by itself, negative current issues from all parts of the structure to be protected. In the case of deep well casings negative current is supplied to the casing head and the current is allowed to distribute itself according to the law of total least resistance. The equations for the exact distribution of a total cathodic protection current, I_p, were derived by Roche [10], providing density profiles for either single or multiple casing strings. Assuming now that using Equation 11 and a casing current profile computed for a given well we have obtained a current density profile, $i_c(z)$, as a function of z and similarly we have calculated the cathodic protection current density distribution, $i_p(z)$, along the entire casing string. The latter will be proportional to the total protection current, I_p, if we ignore the nonlinearities of the overpotentials. As a first move in our determination of the optimal I_p we choose a value sufficiently large so that for all depths z_n the absolute value of the protection current density $|i_p(z_n)| > i_c(z_n)$ or $|i_p(z_n)|/i_c(z_n) > 1$. We next find the minimum value of this ratio, which we shall denote by μ. If our initial choice of the protection current is $(I_p)_0$ then $(I_p)_0/\mu$ is the cathodic protection current that will just cancel all anodic areas of the corrosion current system.

In practice we may be satisfied with a smaller amount of protection, i.e. an amount that reduces the iron loss sufficiently so that failure does not occur during the productive life of the field. One might choose a failure span of forty years for oil wells and as much as eighty years for geothermal wells. As cathodic overprotection carries its own risk of casing embrittlement due to metal hydride formation, it is important to select the smallest amount of protection current that will be economically cost effective.

8. Conclusions

This paper describes the electrochemistry, mathematical physics and numerical analysis related to the evaluation of the principal component of external casing corrosion in deep wells. It presents a procedure for delineating the areas of major corrosive attack and provides a first order estimate of the iron loss rates in these various areas.

The current research has been limited to analyses for unprotected pipe. Future work has to take into account the presence of a cement sheath, polarization in the cathodic areas and a possible multiplicity of casing strings. All of these factors can be handled by extensions of the analytical approach presented here or by the introduction of finite element numerical methods. It seems to be advantangeous to carry out both procedures in parallel, using the analytical solutions to check effects of step size on convergence rates and precision for the finite element techniques. With this preliminary control, the latter can then be extended to apply to cases with discontinuous cement coating and strong variations in the electrical resistivities of the formations penetrated by the well. A guideline has been established for the use of the ultimate results in the calculation of the cathodic protection current required to preserve the casing over the productive life of the well.

Acknowledgements

The author is indebted to Mr Enrique Ernesto Romo Valle and to Dr Mirna Urquidi, who provided the Fortran coding for the computational processes.

He is grateful to the Management of the Instituto de Investigaciones Electricas for the financial and programming aid it has contributed to the research project.

References

[1] H. G. Doll, *Trans. AIME* **179** (1949) 146.
[2] L. de Witte and F. J. Radd, *J. Petroleum Technol.* April 7 (1955) 66.
[3] L. de Witte and K. Fournier, *J. Assoc. Computing Machinery* **5** (1958) 119.
[4] L. de Witte, *Oil Gas J.* 9 May 54 (1955) 109.
[5] T. Teorell, *Proc. Soc. Exptl. Biol. Med.* **33** (1935) 282.
[6] K. H. Meyer and J. F. Sievers, *Helv. Chem. Acta* **19** (1936) 649.
[7] L. de Witte, *AIME, Petroleum Trans.* **204** (1955) 103.
[8] A. Erdelyi, W. Magnus, F. Oberhettinger and F. G. Tricomi, 'Tables of Integral Transforms', Vol. I, (McGraw Hill, New York, 1954) p. 105.
[9] S. P. Frankel, L. de Witte and J. D. Porter, 'Proceedings of the 5th Oil Recovery Conference', Texas Petr. Research Committee, (December, 1952).
[10] M. Roche, *Revue l'Institut Français Pétrole* **32** (1977) 43.